

Indoor Environment in Sickroom with Ceiling Induction Diffusers and Measuring Method of Ventilation Effectiveness Using Tracer Gas

Peihuan Liu *¹, Toshio Yamanaka¹, Ying Li¹, Mari Kuranaga¹

1 Osaka University

2-1 Yamadaoka, Suita City, Osaka, Japan

liupeihuan@arch.eng.osaka-u.ac.jp

ABSTRACT

In order to provide patients with a high quality indoor environment and ensure a pleasant working place for medical care personnel, thermal environment and indoor air quality are regarded as two of the most important requirements.

The authors aimed at the air-conditioning system with ceiling induction diffusers, a kind of unit that prevents draft sensation and reduces energy consumption. In this study, we measured the distribution of concentration of tracer gas from person simulators, temperature distribution, local mean age of air, indoor air velocity and radiation heat transfer in a full scale four-bed sickroom with ceiling induction diffusers under cooling condition.

According to the result, it is found that parameters including the height and position of exhaust vent, pollutant resource position and curtain affect indoor air airflow.

Furthermore, portable infrared absorption CO₂ analyzer, as a carbon dioxide concentration tester was used in this study. It is considered that the responsiveness of CO₂ recorder is strongly related to the experiment results. Thus, how much the responsiveness of CO₂ concentration tester influenced the results was also discussed in this paper.

KEYWORDS

thermal comfort, age of air, tracer gas, step up method, responsiveness characteristic

1 INTRODUCTION

In modern society, with the progress of technology and the development of civilization, the demand for indoor air quality, especially in hospital wards, is also increasing much quickly. Not only for patients, but also for related people including medical staff and accompanying care providers, a high quality indoor air environment does not only guarantee sanitation and comfortable environment for patients, it also reduces the probability of cross-infection, thereby the efficiency and quality of medical work has been improved as well. In normal hospital wards, the pollutant source is generally coming from coughing, patient's excrement, body odor and so on. Even though the traditional ventilation system can provide adequate clean air from outdoor, but due to its airflow pattern, the indoor polluted air and fresh air are mixed and afterwards it might cause the contamination to spread throughout the whole ward. In addition, dry sensation will be easily caused by airflow from diffusers of air-conditioning, especially when the patients can't move freely. Therefore, we introduced induction diffusers of air-conditioning system, which has a kind of outlet with low air velocity and low energy consumption in this study.

The schematic diagram of induction diffuser is shown in Figure 1. Firstly, heated and wet fresh air or cooled and dehumidified fresh air is delivered to air supply chamber. Then, the air is sprayed out at a speed of 3~5m/s through the banding nozzle. As result of negative pressure in air chamber, the indoor air will be induced into the induction chamber. The primary air and indoor air are mixed here and blown out under the action of wind shield cover. The indoor air accounts for 40% and primary air accounts for 60% in total mixed supply air.

In order to observe the indoor airflow characteristic and evaluate indoor air quality under the condition of induction diffusers, we conducted this experiment at imitative wards in Japan.

Meanwhile, in order to evaluate the accuracy of experiment results, an experiment related to responsiveness of CO₂ recorder is also carried out.

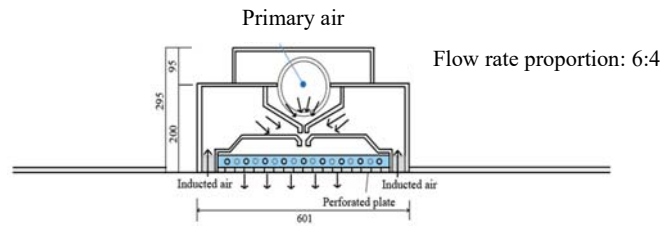


Figure 1. Air-conditioning system with induction panel.

2 IMITATIVE WARDS EXPERIMENT

2.1 Experiment facilities

The experiment was conducted in a full scale imitative ward with four beds (7375mm×5250mm×2420mm). Figure 2 shows the layout of the experiment room. The imitative ward was ventilated by four induction diffusers (1200mm×500mm) which were set above each bed. The total supply airflow rate is about 450m³/h and the exhaust air flow rate is about 380m³/h. The north side wall and east side wall of the room were insulated with polystyrene board (15mm). Near the south side wall, 3 electric carpet were attached to polystyrene board (1000W in total) for simulating heat gain through windows. The simulator of human body (φ300mm×L1500mm) set on each bed was made of spiral duct with polyvinyl chloride (PVC) heating cable, is used to simulate 40W sensible heat caused by human body. As for the heat of furniture like refrigerator and TV in the room, we placed four black lamps (55W×4) at the height of 1000mm above the floor beside each bed. As the experiment was carried out in November, 2017, oil heaters were placed in the machine room to increase the external air to 32°C. The measurement points of temperature and tracer gas concentration were shown in Figure 3. At pole1~pole10, 4 portable infrared absorption CO₂ analyzer set at height of 100mm, 600mm, 1100mm and 1700mm were used to record indoor gas concentration. The time interval of record was 30s. From pole 5 to pole 12, 11 T-thermocouples were set vertically, from pole 5 to pole 12, 10 T-thermocouples were set vertically because of the lack of the highest measurement point due to the beam on the ceiling, as shown in Figure 3 to measure the indoor temperature.

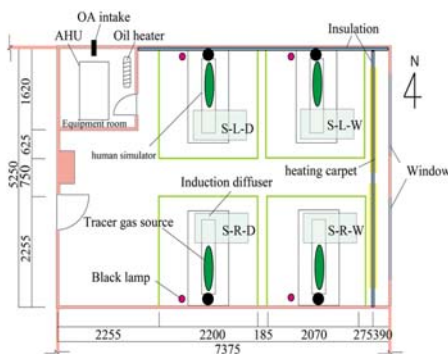


Figure 2. Plan of experiment room.

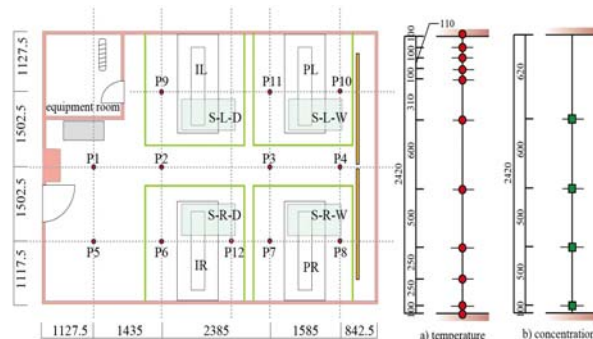


Figure 3. Measurement points.

2.2 Measurement method

The indoor air quality and ventilation effectiveness were evaluated by the index of normalized concentration and local mean age of air. Meanwhile, the radiation heat transfer and air velocity were also measured during the experiment.

■ Normalized concentration measurement

When the indoor air temperature and wall surface temperature became stable, CO₂ (1.5L/min) and He (0.9L/min) gas mixed gas, used as tracer gas, was injected into the experiment room through one or four human body simulators. All of the CO₂ recorders and T-thermocouples recorded the indoor temperature and concentration change until indoor environment reached steady level. In order to examine the impact of exhaust vent position, tracer gas position on the indoor airflow characteristics, experiments under 5 conditions (detailed in Table 1) were carried out in this study.

Table 1. Experimental conditions.

Case	Condition	Exhaust position	Tracer gas position	curtain
Case 1	4EC-PR-C	4EC	PR	○
Case 2	4EC-IR-C	4EC	IR	○
Case 3	4EC-4B-C	4EC	4B	○
Case 4	2EC-4B-C	2EC	4B	○
Case 5	1EC-4B-C	1EC	4B	○

(Note: P: perimeter; I: interior; B: bed; C: with curtain;
 4EC: 4 exhaust vents at the height of 50mm from the ceiling;
 2EC: 2 exhaust vents at the height of 50mm from the ceiling at perimeter and interior side;
 1EC: 1 exhaust vent at the height of 50mm from the ceiling)

The normalized concentration C_n [-] is defined as following Equation (1):

$$C_n = \frac{C_R - C_{OA}}{C_{EA} - C_{OA}} \quad (1)$$

where C_R represents the steady concentration [-], C_{OA} represents the outdoor concentration [-] and C_{EA} represents the exhaust air concentration [-]. Here we assumed $C_R=1$ and $C_{OA}=0$.

■ Local mean age of air measurement

The measurement method is almost the same as Normalized concentration measurement. Only tracer gas was injected through four induction diffusers. With the same aim as the normalized concentration measurement mentioned above, in order to evaluate the impact of exhaust vent height, exhaust vent position, tracer gas position, and curtain on the ventilation effectiveness, we conducted the experiment under 4 conditions. The detailed experimental conditions are given in table 2.

The indoor concentration $C_p(t)$ [-] can be described using the following Equation (2):

$$C_p(t) = \int_0^{\infty} M(t - \tau) R_p(\tau) d\tau = \int_0^{\infty} Q \times C_s(t - \tau) R_p(\tau) d\tau \quad (2)$$

where M [m³/h] is the emission rate of tracer gas, $R_p(t)$ [1/m³] is the impulse responsiveness, τ is the time lag, and $C_s(t - \tau)$ [-] is the concentration of supply air.

Table 2. Experimental conditions.

Item	Condition	Exhaust position	Tracer gas position	curtain
Case 1	4EC-4D-NC	4EC	4D	-
Case 2	4EC-4D-C	4EC	4D	○
Case 3	2EC-4D-C	2EC	4D	○
Case 4	1EC-4D-C	1EC	4D	○

(Note: P: perimeter; I: interior; B: bed; C: with curtain; NC: without curtain;
 4EC: 4 exhaust vents at the height of 50mm from the ceiling;
 2EC: 2 exhaust vents at the height of 50mm from the ceiling at perimeter and interior side;
 1EC: 1 exhaust vent at the height of 50mm from the ceiling)

For obtaining a reasonable $R_p(\tau)$, it is assumed and can be defined via Equation (3),

$$R_p(t) = \begin{cases} b \cdot e^{-c(t-a)}, & x > a \\ 0, & x \leq a \end{cases} \quad (3)$$

where coefficient of a, b, c can be determined using the least squares method.
 The local mean age of air at point p, τ_p [h], is calculated via Equation (4),

$$\tau_p = \frac{\int_0^{\infty} t R_p(t) dt}{\int_0^{\infty} R_p(t) dt} \quad (4)$$

where t is the time [h].

■ Radiation heat transfer measurement

When indoor air environment reached steady state, we measured radiation heat transfer of curtain points at 1100mm height with HUKSEFLUX THERMAL SENSOR (CHF-IRO2) under the condition of 1EC. The measurement points are given in Figure 4. The experiment was carried out under the conditions of “with curtain” and “without curtain”.

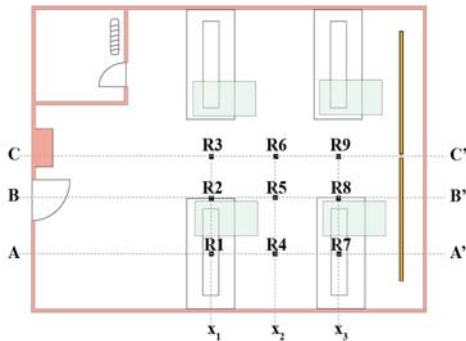


Figure 4. Measurement points (radiation heat transfer measurement).

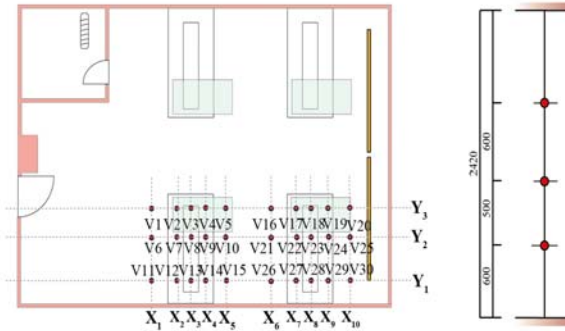


Figure 5. Measurement points (air velocity measurement).

According to the measured result of radiation heat transfer, the mean radiant temperature caused by air beam can be known.

■ Air velocity measurement

When indoor air environment reached steady state, we measured air velocity with a ultrasonic anemometer (DA-700). The measurement point is given in Figure 5. The experiment was carried out under conditions of “with curtain” and “without curtain”.

2.3 Result and discussion

2.3.1 Result of normalized concentration and vertical temperature distribution

The result of vertical temperature distribution is given in figure 6. The temperature differences in every case could be explained by temperature changes of the external air.

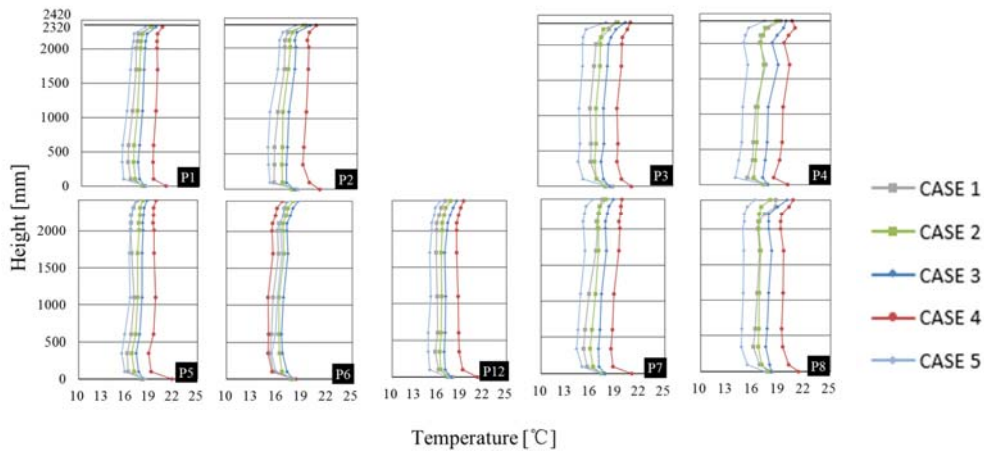


Figure 6. Vertical temperature distribution.

Normalized concentrations in all cases are given in Figure 7. It is obvious that the normalized concentration near pollutant source is particularly high in case 1 and case 2. Comparing case 3, case 4 and case 5, under four exhaust vents condition, the normalized concentration is significantly less than that of other two cases.

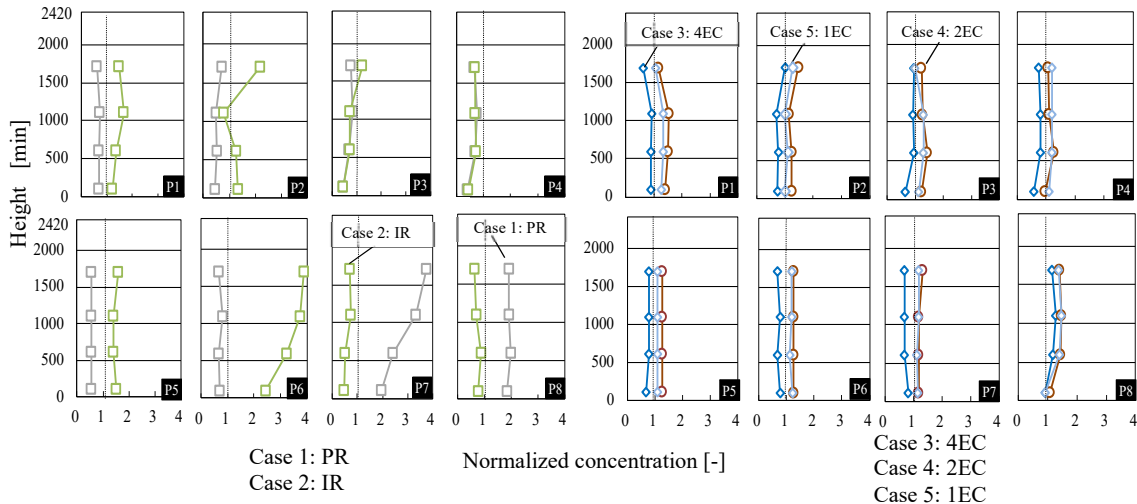


Figure 7. Vertical normalized concentration distribution.

2.3.2 Result of local mean age of air

The result of local mean age of air is showed in Figure 8. When the number of exhaust vents changes, it is shown that the local mean age of air is smaller under the condition of 1EC “with curtain”. At the point of pole 1 and pole 5, the local mean age of air under the condition of “with curtain” is greater than that of “without curtain”, which is because the air flow is harder due to the influence of curtain.

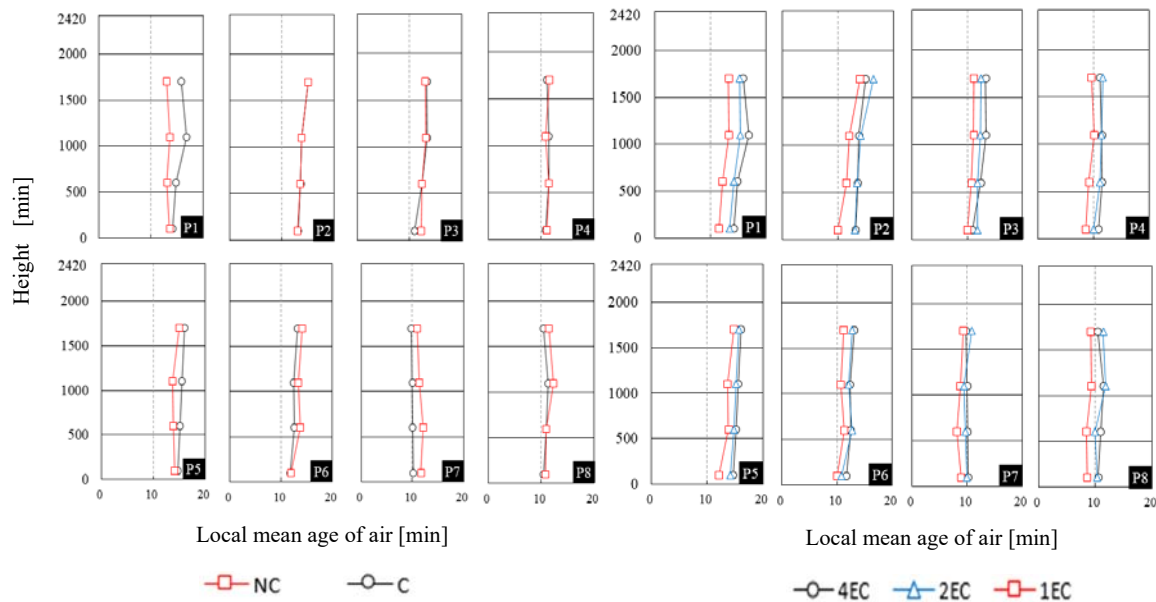


Figure 8. Vertical local mean age of air distribution.

2.3.3 Result of Radiation heat transfer

The indoor air temperature point and radiation temperature of every cross-section are shown in Figure 9. It is shown that the radiation temperature is approximately $0.3^{\circ}\text{C}\sim 0.5^{\circ}\text{C}$ lower than indoor temperature due to radiation heat transfer of diffusers. Beside, due to the carpets on the east side of the room, the radiation temperature increased from X1 section to X3 section.

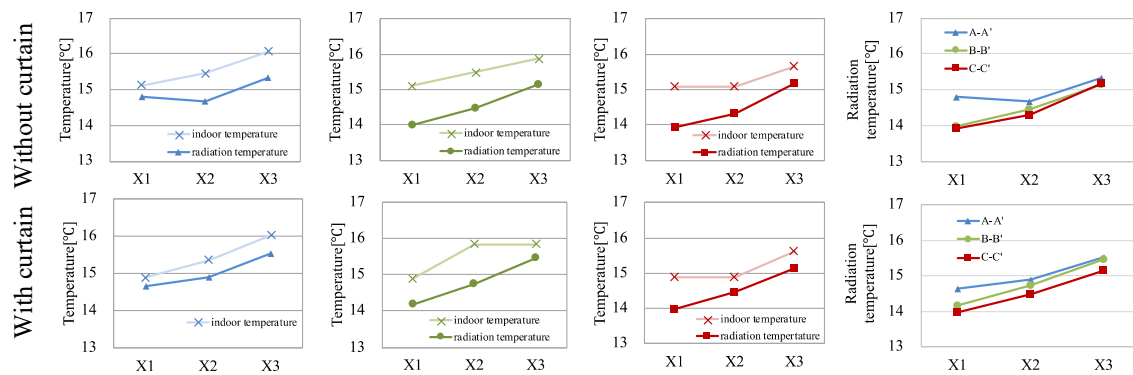


Figure 9. Radiation temperature and indoor air temperature.

2.3.4 Result of air velocity

Figure 10 shows the results of air velocity in X section, Y section and scalar value respectively. At the height of 1700mm, the air velocity is relatively low, less than 0.1m/s . At the height of 1100mm and 600mm, section Y2 and Y3 show the trend that air velocity near S-R-D diffuser is higher than diffuser S-R-W, whereas we can see an opposite result according to section Y1. From Figure 10, we can see that the upward air velocity above human body simulator can be attributed to updraft.

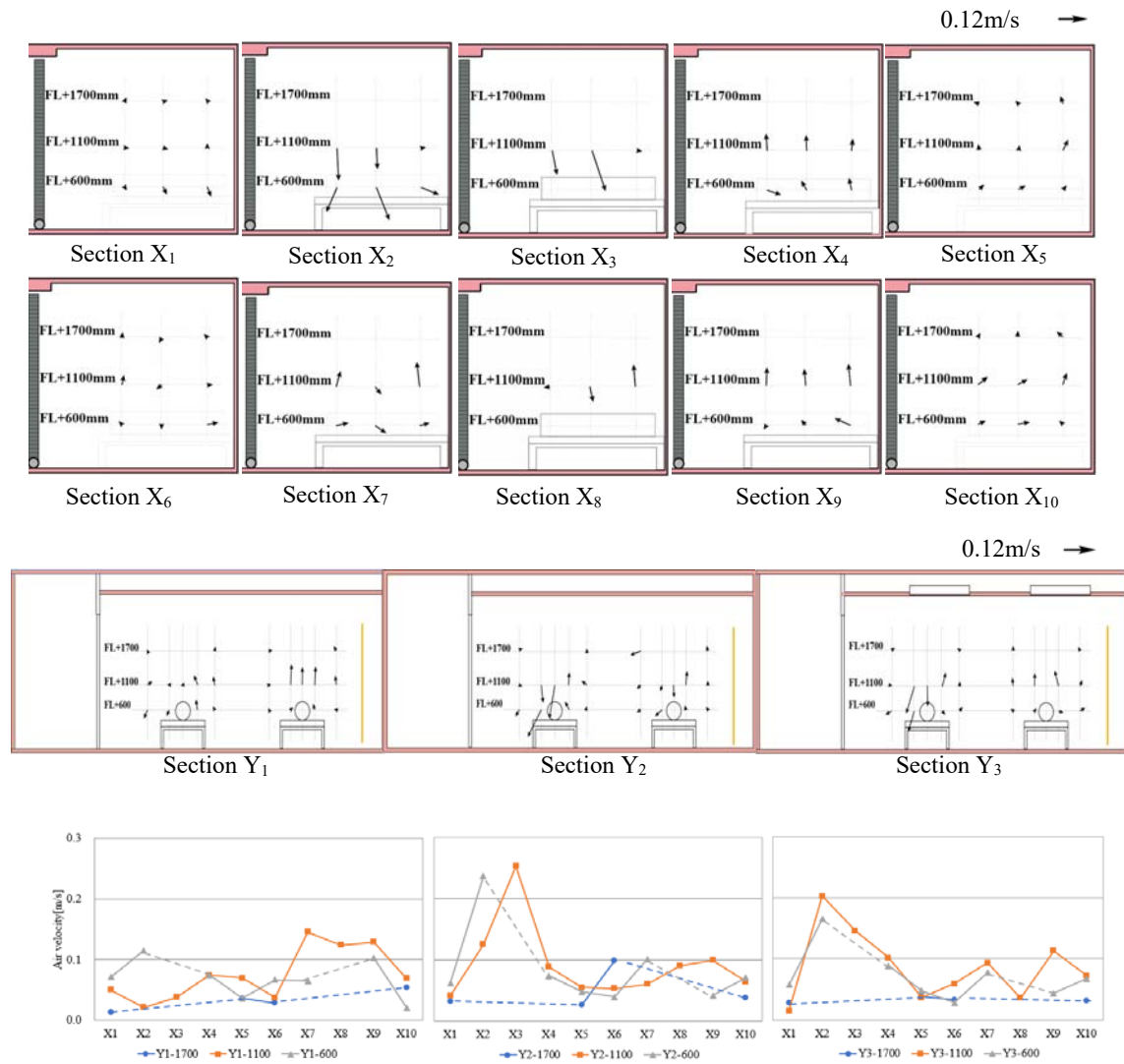


Figure 10. Air velocity result.

3 RESPONSIVENESS CHARACTERISTIC OF CO₂ ANALYZER

3.1 Experiment introduction

During the experiment above, all the concentration data were recorded by portable infrared absorption CO₂ analyzer. It seems that each recorder has its own responsiveness characteristic and it may influence the experimental results to a certain extent. In order to

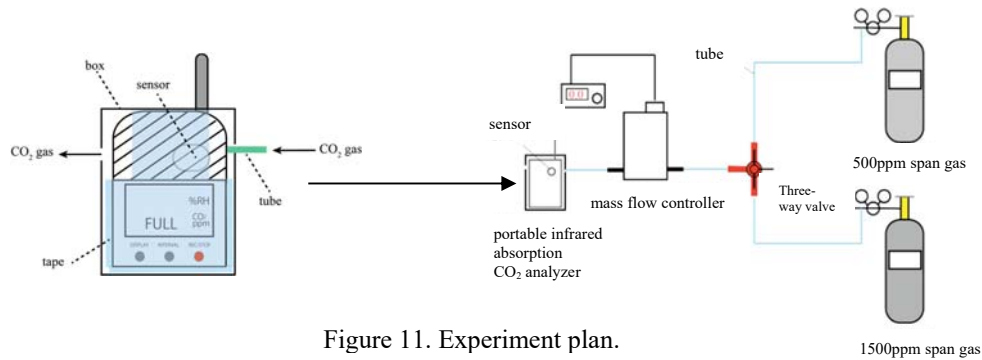


Figure 11. Experiment plan.

evaluate the effect of responsiveness of CO₂ analyzer on the measurement result, we conducted the experiment to evaluate the effect of responsiveness on the measured CO₂ concentration. The schematic of the experimental set-up is shown in Figure 11. Experiment conditions are given in Table 3.

Table 3. Experiment conditions.

Case	Facility	Injecting method	Measurement method	tape	Injecting flow rate [L/min]	Injecting concentration[ppm]	
1	Box	Forced injection	Step up	○	0.27~4.32	1491	503
2	vinyl bag	Forced injection	Step up	—	4.32	1491	503
3	vinyl bag	Forced injection	Step down	—	4.32	1491	503
4	vinyl bag	Natural injection	Step down	—	—	1491	≈455

In Case 1,2 and 3, a CO₂ analyzer was put in a box or a vinyl bag. Using 503ppm and 1491ppm span gas cylinder, CO₂ gas of different concentration was injected to box or vinyl bag interchangeably. We examined the step change process of CO₂ concentration until steady state. Besides, in Case 1, CO₂ gas was injected at different flow rates. We found that when flow rate is 4.32L/min, the result was relatively accurate. Therefore, for Case 2 and 3, the experiments were all conducted under this flow rate 4.32L/min. In Case 4, after the CO₂ recorder was put into a vinyl bag, we injected 1491ppm gas to the bag until the concentration in bag reached a steady state. Then the CO₂ analyzer was quickly taken out from the bag and be exposed to the air in the experimental room. Then a decay process of the concentration was observed. The image of the experimental procedure is shown in Figure 12 for all four cases.

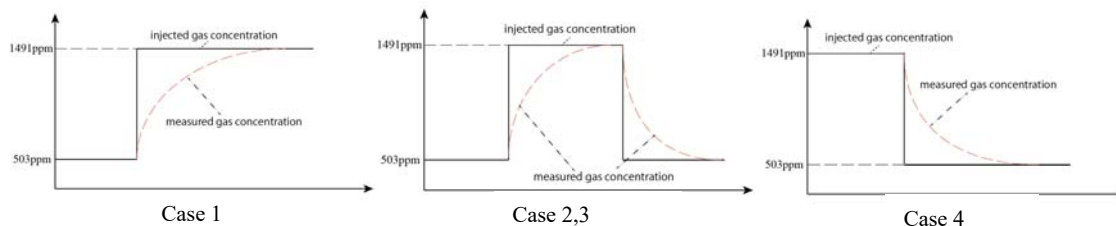


Figure 12. Experiment process.

3.2 Results and discussion

Measured concentration of Case 1 under different flow rates is given in Figure 13. Using the average value of three-time measurements under 4.32L/min, differential value and its moving average value is shown in Figure 14.

Comparing 4 cases, their measured concentration and moving average value of 5 seconds are given in Figure 15 and Figure 16, respectively.

Here, we assumed an approximate curve model as shown by Equation (5):

$$f(x) = \begin{cases} ax^i e^{-bx}, & x \leq \frac{i}{b} \\ ax^j e^{-dx}, & x > \frac{i}{b} \end{cases} \quad (5)$$

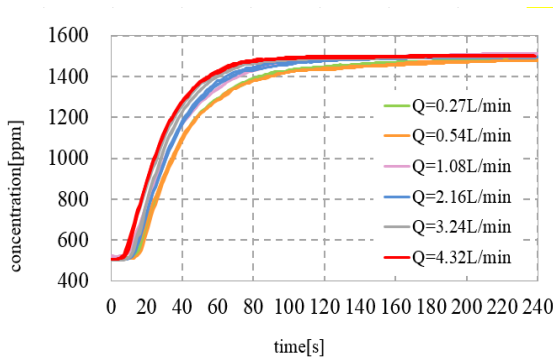


Figure 13. Measure concentration (case 1)

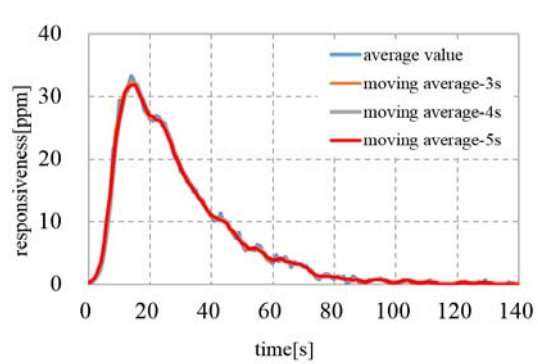


Figure 14. Differential value (case 1)

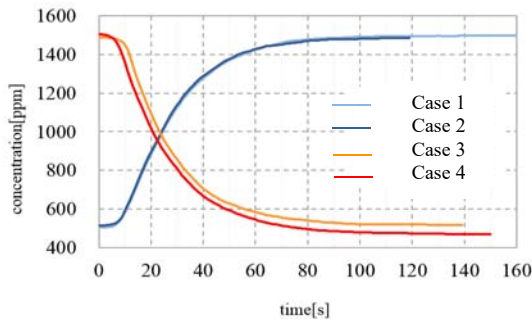


Figure 15. Measure concentration (case 1~4)

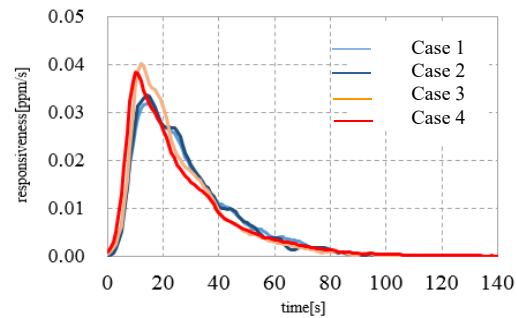


Figure 16. Differential value (case 1~4)

As x becomes i/b when responsiveness reaches the highest point, then the coefficient of “a” and “b” can be decided according to responsiveness data.

The comparison of the approximate curve model and moving average value of 5 seconds in each case is shown in Figure 17.

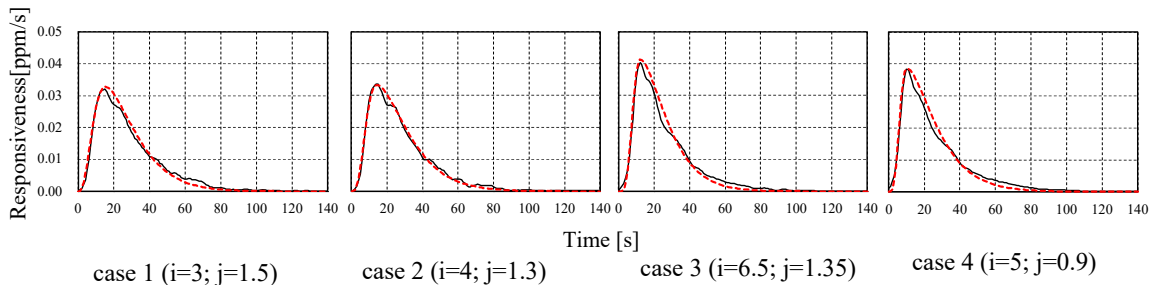


Figure 17. Approximate curve.

— Moving average-5s
- - - approximation

For imitating the change process of indoor concentration, the difference method is used. Assuming calculated indoor concentration is the true value of indoor air concentration, and the responsiveness of CO₂ recorder is defined as R(t), then the measured CO₂ concentration can be calculated via Equation (6):

$$C_p(t) = \int_0^{\infty} \frac{C(t - \tau)R(\tau)}{\Delta C} d\tau \quad (6)$$

where $C_p(t)$ is the measured indoor concentration [-], C is the calculated indoor concentration [-], and t, τ is the time [s].

Figure 18 shows the result of calculated concentration (true value) and measured concentration of Case 1 and Case 4 under different air changes. Figure 19 illustrates the comparison results of measurement concentration using approximate value and responsiveness of Case 1.

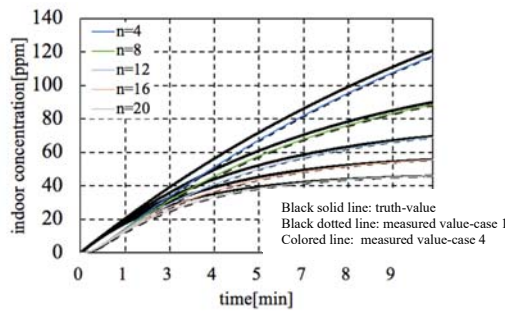


Figure 18. Results review of case 1 and case 4

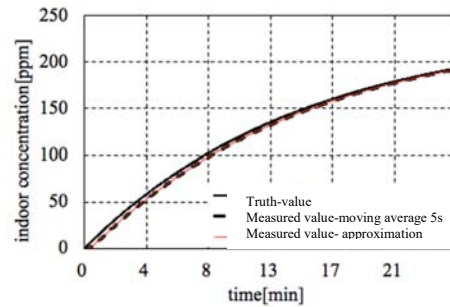


Figure 19. Results review of approximate curve (case 1)

During the first minute, the delay time between the calculated true value and measured value is roughly the same under each air change. As time goes on, the greater the air change is, the shorter the delay time is. According to Figure 19, it is considered that the result of approximate value is consistent with the result of Case 1.

4 CONCLUSIONS

In this study, the knowledge were obtained and summarized as follows,

- Near the pollutant sources, the normalized concentration is much higher than other measurement points.
- The normalized concentration under 4 exhaust vents condition is the lowest.
- The local mean age of air under 1 exhaust vent is the lowest.
- Curtains can influence the air flow out when exhaust vents are inside of the curtain.
- The induction diffusers do have radiation effect.
- The remaining time of deviation decreases as the as the air change rate increases.

5 ACKNOWLEDGEMENTS

This study is supported by KIMURA KOHKI corporation and the author would like to thank professor KOTANI who provided valuable advice and guidance in the period of time during his life while living.

6 REFERENCES

1. KURANAGA Mari, YAMANAKA Toshio, KOTANI Hisashi, MOMOI Yoshisa, SAGARA Kazunobu, LI Ying: Controlling Method of Indoor Environment in Sickroom with Ceiling Induction Diffusers, (part 4) Influence of Exhaust Position on Indoor Environment in Sickroom with Four Beds under Cooling Condition with All Fresh Air. *Proc. AIJ research meeting, 2017.8*
2. MOMOI Yoshihisa, UGIYAMA Akifumi: Effect of sensor Response Speed on Measurement Accuracy of Air Change Rate in Tracer Gas Decay Method, part 1, Prediction of sensor Response by Convolution Intergration. *Proc. AIJ Kinki Chapter research meeting, 2018.6*